UCSF
UC San Francisco Previously Published Works

Title

Meiotic onset is reliant on spatial distribution but independent of germ cell number in the mouse ovary

Permalink

https://escholarship.org/uc/item/0b38c09x

Journal

Journal of Cell Science, 129(13)

ISSN

0021-9533

Authors

Arora, Ripla
Abby, Emilie
Ross, Adam DJ
et al.

Publication Date

2016-07-01

DOI

10.1242/jcs.189910

Peer reviewed

eScholarship.org Powered by the California Digital Library
University of California

© 2016. Published by The Company of Biologists Ltd | Journal of Cell Science (2016) 129, 2493-2499 doi:10.1242/jcs.189910

SHORT REPORT

Meiotic onset is reliant on spatial distribution but independent of germ cell number in the mouse ovary

Ripla Arora[1,*], Emilie Abby[2,*], Adam D. J. Ross[1], Andrea V. Cantu[1], Michael D. Kissner[1], Vianca Castro[1], Hsin-Yi Henry Ho[3], Gabriel Livera[2] and Diana J. Laird[1,‡]

ABSTRACT

Mouse ovarian germ cells enter meiosis in a wave that propagates from anterior to posterior, but little is known about contribution of germ cells to initiation or propagation of meiosis. In a *Ror2* mutant with diminished germ cell number and migration, we find that overall timing of meiotic initiation is delayed at the population level. We use chemotherapeutic depletion to exclude a profoundly reduced number of germ cells as a cause for meiotic delay. We rule out sex reversal or failure to specify somatic support cells as contributors to the meiotic phenotype. Instead, we find that anomalies in the distribution of germ cells as well as gonad shape in mutants contribute to aberrant initiation of meiosis. Our analysis supports a model of meiotic initiation via diffusible signal(s), excludes a role for germ cells in commencing the meiotic wave and furnishes the first phenotypic demonstration of the wave of meiotic entry. Finally, our studies underscore the importance of considering germ cell migration defects while studying meiosis to discern secondary effects resulting from positioning versus primary meiotic entry phenotypes.

KEY WORDS: Meiosis, Wave, Gonad, Germ cell, Migration, Ror2

INTRODUCTION

Reproduction relies on meiosis, a cell division program for deriving gametes from diploid precursors known as primordial germ cells. Female germ cells enter meiosis during fetal development whereas males defer until after birth (Spiller and Bowles, 2015). Meiosis initiates asynchronously in mammalian ovaries, spanning >24 h in mice, and months in humans (Hunt and Hassold, 2008; Spiller and Bowles, 2015). In female mice, meiosis initiates at embryonic day (E)13.5 in a wave-like pattern, with germ cells located at the anterior end expressing markers of commitment (Menke et al., 2003; Yao et al., 2003; Bullejos and Koopman, 2004; Koubova et al., 2006, 2014). Upregulation of SYCP3 similarly ensues, marking the initiation of meiotic prophase I, which comprises leptotene, zygotene, pachytene and diplotene. Expression of pluripotency factor OCT4 (also known as POU5F1) is concomitantly quenched in an anterior to posterior wave (Bullejos and Koopman, 2004). To date, evidence confirming the wave of meiosis consists of gene expression changes in an anterior–posterior manner.

Two hypotheses explain the stereotypical wave of meiotic entry; the intrinsic clock model maintains that germ cells undergo a defined number of mitotic divisions, such that the first to proliferate initiate meiosis first (Ohkubo et al., 1996; McLaren and Southee, 1997; McLaren, 2003). Alternatively, in the morphogen model a diffusible meiosis-inducing factor (MIF) must reach the anterior of the ovary first to produce a wave. A prime candidate MIF is retinoic acid, which diffuses in from the mesonephros (Bowles et al., 2006), although retinoic-acid-independent mechanisms have also been proposed (Kumar et al., 2011).

Although it has been insinuated that the meiotic wave is a byproduct of germ cell migration (Menke et al., 2003; Bullejos and Koopman, 2004), there is no evidence that first meiotic entrants at the anterior ovary migrated farthest or most efficiently (Molyneaux et al., 2001). In apoptosis-resistant *Bax* mutants, ectopic germ cells located furthest anterior (in the adrenals) enter meiosis first, whereas the posterior ectopic germ cells (in the tail) are least differentiated (Runyan et al., 2008); this suggests that meiotic entry is tied to location, resulting from either intrinsic germ cell differentiation or proximity to the source of MIF.

Wnt signaling has been implicated in germ cell development and sex differentiation in mammals. Ovarian somatic cells rely on Wnt4 and its effector β-catenin for female sex differentiation and entry of germ cells into meiosis (Vainio et al., 1999; Ottolenghi et al., 2007; Liu et al., 2009). In the absence of signaling, gonad somatic cells adopt a male fate, driving male differentiation in some germ cells, whereas those entering meiosis are delayed (Vainio et al., 1999; Liu et al., 2010; Naillat et al., 2010; Chassot et al., 2011). Signaling mediated by Wnt5a and its receptor Ror2 is key during germ cell migration and disruption of either diminishes the efficiency with which germ cells populate the gonads (Laird et al., 2011; Chawengsaksophak et al., 2012). Ror2 expression in the gonad increases dramatically at the time of sex differentiation (Arora et al., 2014), whereas Wnt5a expression concomitantly becomes restricted to the testis (Chawengsaksophak et al., 2012).

Here, the study of two Ror2 mutants connects aberrant germ cell migration to defects in meiosis and supports the diffusion model of meiotic entry.

RESULTS AND DISCUSSION

Reduced proportion of meiotic germ cells in *Ror2* mutants

Prompted by a sharp increase in *Ror2* transcript levels coincident with sex differentiation and subsequent decline in mouse female germ cells (Arora et al., 2014), we examined fetal gonads in a point mutant ($Ror2^{Y324C}$, Laird et al., 2011). $Ror2^{Y324C/Y324C}$ ovaries were smaller and contained significantly fewer germ cells (Fig. 1A–D; Fig. S1A) compared with age-matched controls (WT, includes

[1]Department of Ob/Gyn and Reproductive Sciences, Eli and Edythe Broad Center for Regeneration Medicine and Stem Cell Research, University of California, San Francisco, 35 Medical Center Way, San Francisco, CA 94143, USA. [2]University Paris Diderot, Sorbonne Paris Cite, Laboratory of Development of the Gonads; CEA, DSV, iRCM, SCSR, LDG; INSERM, Unit of Genetic Stability, Stem cells and Radiation, UMR-967; University Paris-Sud, Fontenay-aux-Roses F-92265, France. [3]Department of Cell Biology and Human Anatomy, University of California, Davis School of Medicine, 4422 Tupper Hall, Davis, CA 95616, USA.
*These authors contributed equally to this work

‡Author for correspondence (diana.laird@ucsf.edu)

E.A., 0000-0003-0284-4760; M.D.K., 0000-0001-7603-2402; D.J.L., 0000-0002-4930-0560

Received 31 March 2016; Accepted 13 May 2016

Journal of Cell Science

Journal of Cell Science (2016) 129, 2493-2499 doi:10.1242/jcs.189910

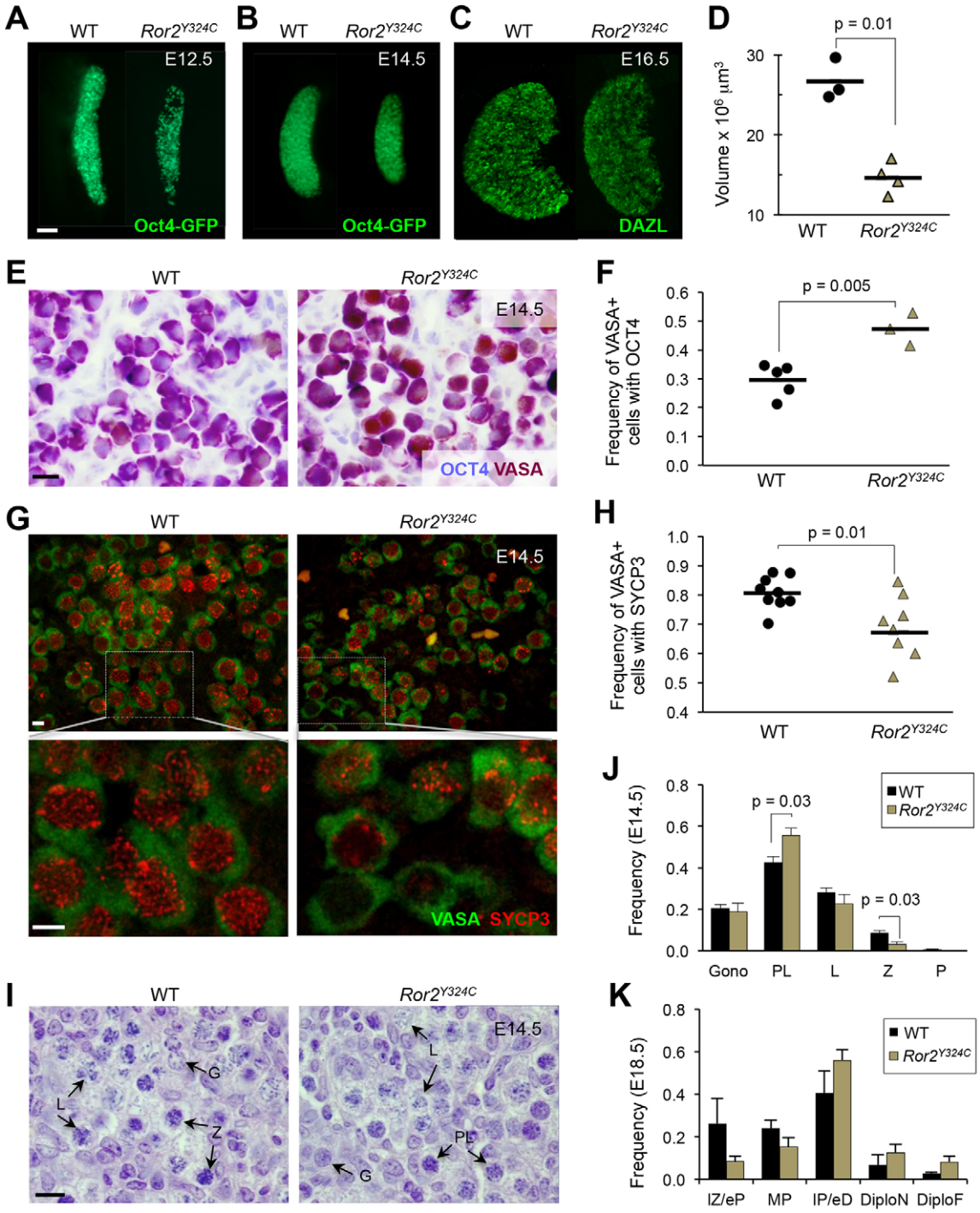

Fig. 1. Meiotic entry is delayed in *Ror2*$^{Y324C/Y324C}$ ovaries. (A–D) Smaller ovaries and diminished germ cells in *Ror2*$^{Y324C/Y324C}$; Oct4–GFP at E12.5 (A), E14.5 (B), and DAZL at E16.5 (C) and volume measurement (D, *P*=0.01, *t*-test). (E,F) Higher frequency of VASA+ OCT4+ germ cells in mutant ovaries (*P*=0.005, *t*-test). (G,H). Lower frequency of SYCP3+ germ cells in mutant ovaries (*P*=0.01, *t*-test). (I) H&E sections of E14.5 ovaries. Arrows indicate stages of meiotic prophase. (J,K) Quantification of I. *n*=6 at E14.5 (J) and *n*=3 at E18.5 (K). Data represented as mean±s.e.m. G/Gono, gonocytes; PL, pre-leptotene; L, leptotene; Z, zygotene; P, pachytene; lZ/eP, late-zygotene/early-pachytene; MP, mid-pachytene; lP/eD, intermediate-pachytene/early-diplotene; DiploN, naked-diplotene; DiploF, diplotene-forming follicle. Scale bars: 100 µm in A–C; 10 µm in E,G,I.

phenotypically wild-type and heterozygous animals). Although migration-mediated loss of *Ror2*$^{Y324C/Y324C}$ germ cells by E11.5 was previously established (Laird et al., 2011), persistence until E14.5 indicates that proliferation does not compensate for this reduction. Among germ cells that reach *Ror2*$^{Y324C/Y324C}$ ovaries, the proportion in meiosis at E14.5 was reduced, as assessed by retention of OCT4 (Fig. 1E,F) and onset of SYCP3 (Fig. 1G,H). This meiotic delay was supported by reduced *Sycp3*, *Stra8* and *Spo11* transcripts in *Ror2*$^{Y324C/Y324C}$ germ cells at E13.5 (Fig. S1B) and nuclear morphology at E14.5, which revealed an increased proportion of germ cells at preleptotene stage in *Ror2*$^{Y324C/Y324C}$ and a decreased proportion at zygotene compared with WT (Fig. 1I,J and Table S1). Delayed initiation did not affect progression of meiosis, as comparable numbers of germ cells were found across meiotic

Journal of Cell Science

Journal of Cell Science (2016) 129, 2493-2499 doi:10.1242/jcs.189910

stages at E18.5 (Fig. 1K). Thus, histology and expression studies corroborate a delay in meiotic initiation at a population level in *Ror2*$^{Y324C/Y324C}$ ovaries. Perinatal lethality of *Ror2*$^{Y324C/Y324C}$ embryos (Laird et al., 2011) and inefficient conditional deletion of the *Ror2* locus (data not shown) precluded analysis of postnatal oocyte and ovary development.

Meiotic initiation is independent of germ cell number

Given the overall phenotypic similarity between two *Ror2* alleles (DeChiara et al., 2000; Takeuchi et al., 2000; Laird et al., 2011), we analyzed ovaries from knockouts. *Ror2*$^{-/-}$ ovaries were also smaller than WT controls and the number of germ cells was decreased (Fig. 2A). Most *Ror2*$^{-/-}$ ovaries showed a meiotic entry profile similar to WT (Fig. 2B), however a reduced frequency of SYCP3+ germ cells was observed in one of five knockout ovaries similar to *Ror2*$^{Y324C/Y324C}$. The same *Ror2*$^{-/-}$ ovary exhibited a severe diminution of germ cells. When all mutants and WT littermates were considered, a significant correlation was found between germ cell number per section and overall frequency of SYCP3 expression (Fig. 2B; r=0.605, P=0.0013) suggesting that either germ cell loss or else severity of the mutant phenotype caused the observed delay in meiotic initiation in mutants.

To test if a threshold quantity of germ cells is required for proper initiation of meiosis, we chemically depleted germ cells *in vivo* using busulfan. VASA+ germ cells from treated litters were evenly dispersed throughout the ovary (Fig. 2C). At E14.5, although busulfan-mediated reduction in germ cells (across CD1 and FVB genetic backgrounds) approximated the most severe *Ror2* mutants, the overall frequency of meiotic germ cells did not differ from untreated controls (Fig. 2D,E). These results rule out the possibilities that a critical number of germ cells is required to relay MIFs to act permissively for somatic cells to deliver such signals.

Meiotic delay in *Ror2* mutants is not caused by sex reversal

To assess somatic sex differentiation in *Ror2* mutant ovaries, we compared transcript levels of female markers *Wnt4*, *Foxl2* and *Rspo1* at E12.5 (Fig. S2A) and granulosa cell number and distribution by FOXL2 staining at E14.5 (Fig. S2B–D), but no detectable differences were found. We examined *Sox9* at E12.5 (Fig. S2A), 3βHSD and AMH at E14.5 (Fig. S2E, data not shown), however, no male markers were detected in *Ror2*$^{Y324C/Y324C}$ ovaries. Thus, the delay in meiotic entry in *Ror2*$^{Y324C/Y324C}$ germ cells is not explained by the loss of female somatic sex differentiation or ectopic male somatic differentiation.

Aberrant germ cell distribution causes a population-level delay in meiotic entry but initiation is normal relative to position

Although meiotic delay in most severe *Ror2* mutants is not attributable to low germ cell number, a preferential loss of germ cells at the anterior extreme in approximately half of *Ror2*$^{Y324C/Y324C}$ ovaries (Table S2) and one *Ror2*$^{-/-}$ (Fig. 2B,F) coincided with the meiotic delay (Table S3). Anterior germ cell deficiency was apparent in the testes (data not shown) as well as the ovary following colonization of the gonad at E12.5 (Fig. 2G). Ovaries with loss of germ cells in the anterior might simply lack the first meiotic entrants (Fig. 2H), which manifests as a delay when assessed at the population level. Somatic gonad differentiation was not disrupted in the anterior region of *Ror2*$^{Y324C/Y324C}$ ovaries, as revealed by whole gonad immunostaining for FOXL2 (Fig. S3A) and PECAM (Fig. S3B).

To determine if aberrant positioning of germ cells skews meiotic initiation, we staged prophase I in *Ror2*$^{Y324C/Y324C}$ mutants in conjunction with the position of each germ cell on the anterior–posterior axis. We partitioned sagittal sections of E14.5 ovaries into quadrants, with Q1 being the furthest anterior and Q4 being the most posterior, and scored nuclear morphology of germ cells in each compartment (Fig. 3A,B). Whereas germ cells were nearly equally distributed across quadrants in WT, a relative skewing away from Q1 and Q2 in *Ror2*$^{Y324C/Y324C}$ ovaries (Fig. 3C) is consistent with the anterior depletion observed in Fig. 2. Despite these differences, the frequencies of germ cells in pre-leptotene, leptotene and zygotene stages were similar between mutant and WT in the first two anterior quadrants (Fig. 3D), indicating that the wave of meiotic entry is preserved when germ cells are diminished and mislocalized.

Given the potential discrepancy in the quadrant sizes for mutants with smaller ovaries, we measured the absolute distance from every germ cell to the anterior tip of the ovary in each section. In WT, a strong correlation between meiotic stage and distance from the anterior (r=0.869, P<0.0001) reflects the established anterior–posterior wave of meiotic initiation (Fig. 4A). In *Ror2*$^{Y324C/Y324C}$ ovaries, distances were identical to WT for preleptotene, leptotene and zygotene stages; however, a complete loss of pachytene is concordant with a depletion of germ cells at the anterior tip (Fig. 4A). Most notably, the distance to gonocytes (pre-meiotic germ cells) was significantly shorter in *Ror2*$^{Y324C/Y324C}$ ovaries (Fig. 4A). This result corroborates proper scheduling of meiotic entry according to position in mutants; reduced anterior–posterior distance of gonocytes reflects a truncated gonad length, as measured distances in *Ror2*$^{Y324C/Y324C}$ did not exceed 450 µm, whereas distances up to 600 µm were found in WT. To model this posterior truncation, we removed all germ cells in the WT dataset located >450 µm from the most-anterior end of the ovary. The resulting simulation recapitulated the reduced mean distance to gonocytes observed in *Ror2*$^{Y324C/Y324C}$ (Fig. 4B). Together, these anterior–posterior measurements and modeling the absent posterior extreme of the gonad corroborate the hypothesis that aberrant timing of meiotic entry in *Ror2*$^{Y324C/Y324C}$ ovaries results from defects in the distribution of germ cells as well as gonad morphology.

Ror2 mutant phenotypes link germ cell migration to meiotic initiation

Anterior depletion of germ cells in *Ror*2 ovaries is likely a consequence of earlier migration defects. Despite absent Wnt5a expression in the fetal ovary (Chawengsaksophak et al., 2012), similar anterior loss of germ cells in the *Wnt5a* null gonads (data not shown) supports this idea. Strikingly, *Sfrp1/2* double knockout produces an anterior germ-cell defect in the testis (Warr et al., 2009), highlighting the role of Wnt signaling in germ cell migration as well as the persistence of early migration defects into sex differentiation.

The relationship between migration and positioning of germ cells in the gonad remains unclear. Germ cell movement along the embryonic anterior–posterior axis is believed to occur passively within the extending hindgut (Buehr et al., 1993; Molyneaux et al., 2001), and subsequent migration occurs in the dorsal and lateral directions. Upon colonizing the gonad, germ cells proliferate more rapidly and lose their capacity to migrate (Di Carlo and De Felici, 2000; Kierszenbaum and Tres, 2001). Hence, the absence of germ cells in the gonad anterior could result from an earlier restriction in anterior extension of the hindgut (Fig. 4C,D). Our observations of *Ror2* mutants are the first to connect migratory defects to colonization of a specific region of the gonad.

Journal of Cell Science (2016) 129, 2493-2499 doi:10.1242/jcs.189910

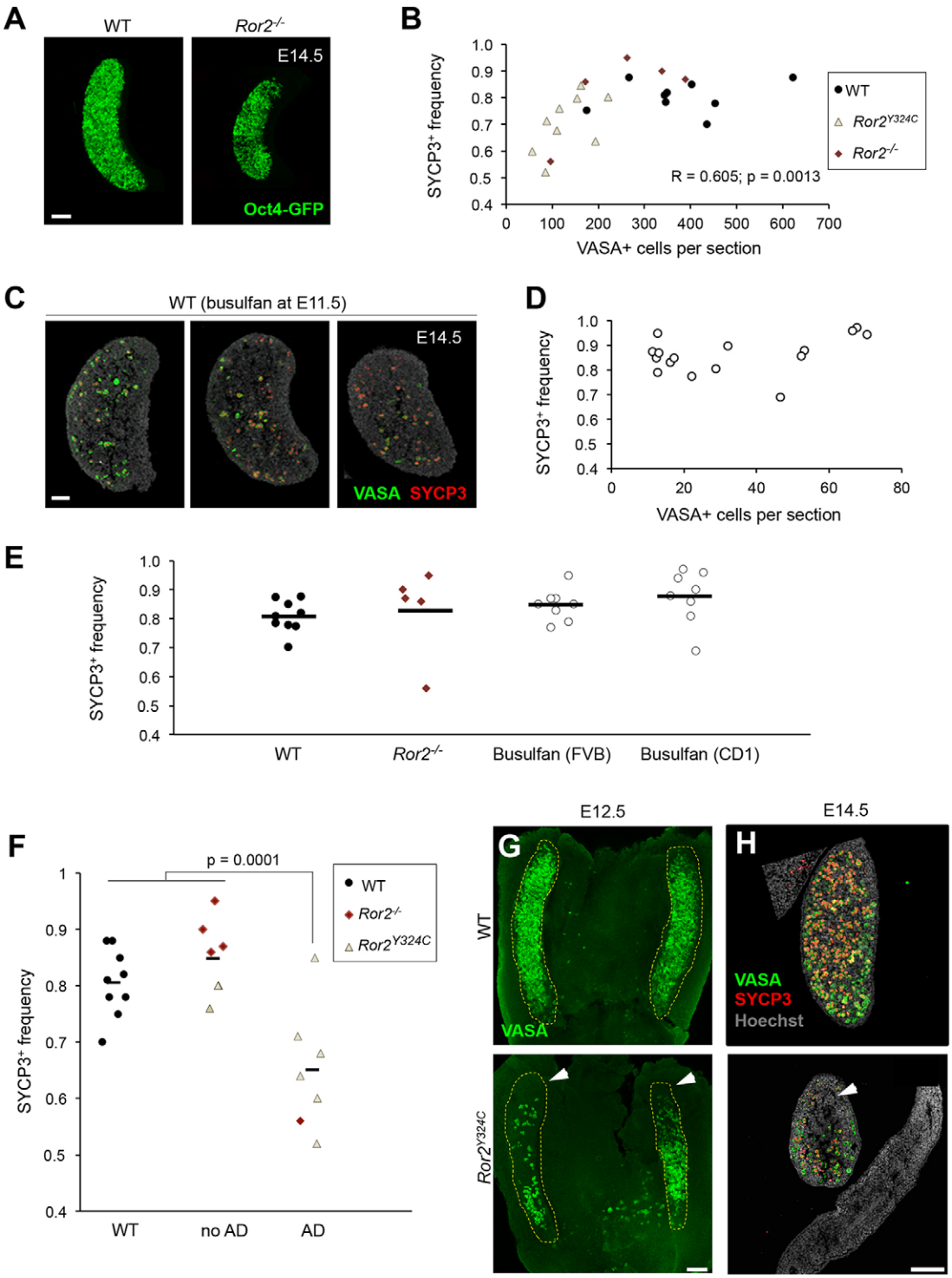

Fig. 2. Diminished number of germ cells does not delay meiotic initiation. (A) Smaller size and reduced number of germ cells (Oct4–GFP) in whole *Ror2*$^{-/-}$ ovaries. (B) Scatter plot shows correlation (r=0.605, *P*=0.0013) between number of germ cells (VASA+) per section and frequency of SYCP3+ germ cells. (C) Busulfan-treated ovary sections. (D) Frequency of SYCP3+ germ cells at E14.5 did not decrease in busulfan-treated ovaries. (E) Percentage of SYCP3+ germ cells was similar between WT, *Ror2*$^{-/-}$ and busulfan treatment. (F) Data in Fig. 2B re-plotted, segregating ovaries with and without anterior defect (AD) in *Ror* mutants. (G) Anterior depletion of germ cells (VASA, green) in *Ror2*^{Y324C} mutants. (H) Sagittal sections show germ cells (VASA, green) that have entered meiosis (SYCP3, red) at E14.5. White arrowheads, anterior defects. Images are oriented with anterior at the top. Scale bars: 100 µm in A,G,H; 50 µm in C.

Migration mutants favor gradient hypothesis

According to the intrinsic clock model, appropriate meiotic entry by anterior–posterior location observed in *Ror2* mutants could be maintained only if the oldest germ cells destined for the anterior extreme of the gonad entirely failed to reach their target. This requirement is inconsistent with our observations of *Ror2* extragonadal germ cells in variable locations along the anterior–posterior axis, not exclusively in the anterior (Fig. S3C). The diffusible signal model of meiotic initiation more congruously explains the correct entry when indexed by location in *Ror2* mutants

Journal of Cell Science

Journal of Cell Science (2016) 129, 2493-2499 doi:10.1242/jcs.189910

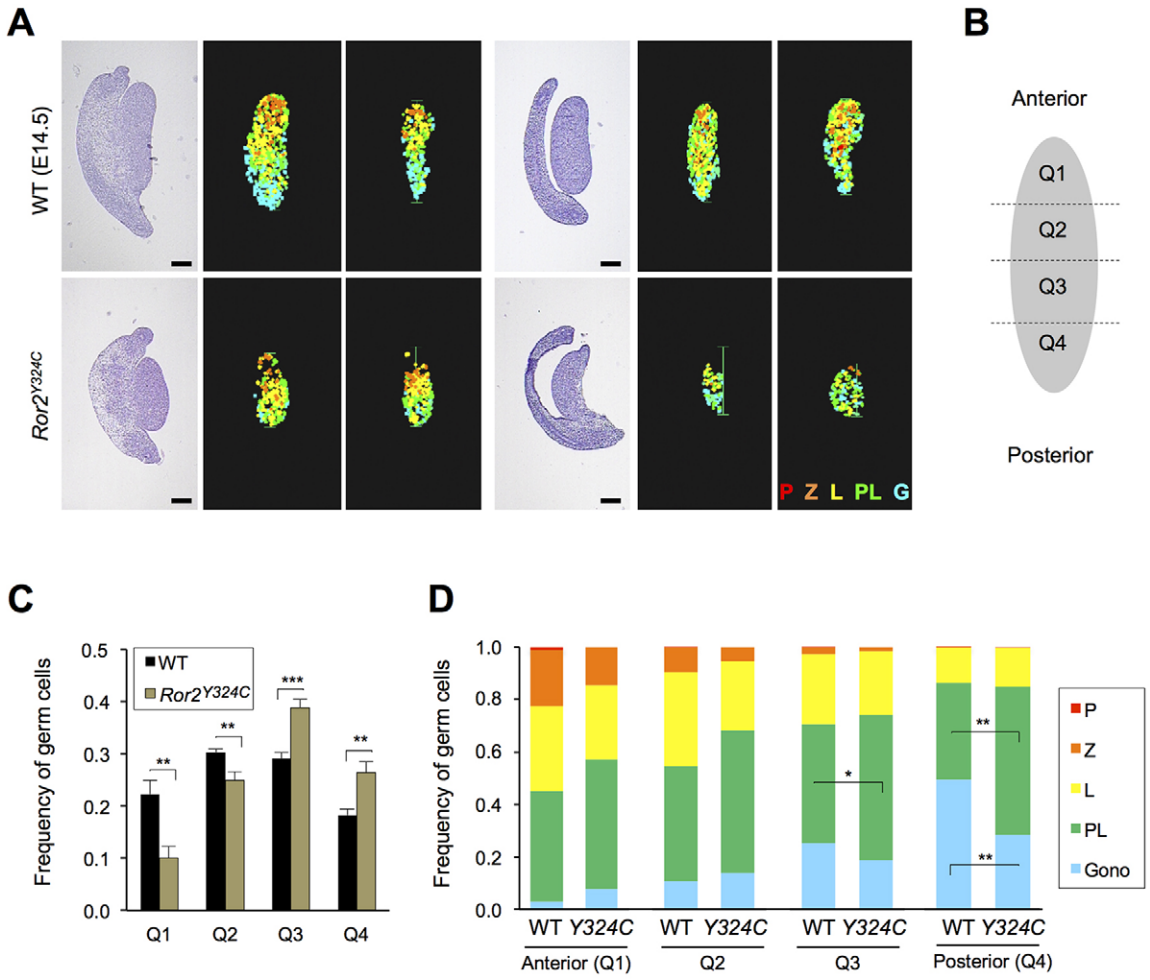

Fig. 3. Aberrant distribution of germ cells in the ovary causes meiotic entry defect. (A) Histologic sections with H&E stain at left and heat maps indicating meiotic progression on right. (B) Diagram showing division of ovaries into quadrants. (C) Relative frequency of germ cells counted in each quadrant in WT versus *Ror2*$^{Y324C/Y324C}$, *n*=6 embryos. Data represented as mean±s.e.m. (D) Distribution of germ cells scored in each stage of meiotic prophase for each quadrant, *n*=6 WT and *n*=6 *Ror2*$^{Y324C/Y324C}$ ovaries. Gono, gonocytes; PL, preleptotene stage; L, leptotene stage; Z, zygotene stage; P, pachytene stage. ***P<0.001, **P<0.01, *P<0.05 by *t*-test. Scale bars: 200 µm.

with aberrant germ cell distributions (Fig. 4D). Our data support the model of a MIF that travels from the anterior to the posterior extreme of the ovary. Confirmation of this hypothesis must await more sophisticated lineage labeling and time-lapse imaging of germ cells with heterogeneous migration trajectories.

Our studies suggest that germ cell migration mutants could be tools to further explore consequences of disruption to the anterior–posterior wave of meiosis. We highlight a need to rule out migration defects while studying meiosis to discern secondary effects resulting from positioning versus primary meiotic entry phenotypes. Finally, we conclude that neither germ cell number, nor localized loss of germ cells in the anterior ovary, affects the wave of meiotic entry, supporting a strong role for the niche and somatic gonad in driving sex differentiation and meiotic initiation in the ovary.

MATERIALS AND METHODS

Mice

Ror2$^{Y324C/Y324C}$ (Laird et al., 2011) and *Ror2*$^{-/-}$ (Arora et al., 2014) mice were mated with Oct4-ΔPE eGFP (Oct4–GFP) (Boiani et al., 2004) to label germ cells. Busulfan (Sigma, B2635) (Douglas et al., 2013) was injected intraperitoneally (20 mg/ml in 40 µl) in pregnant E11.5 CD1 or FVB females crossed with C57/Bl6;Oct4-GFP males. Embryos were dissected from timed matings and tails genotyped by PCR. The dark period was 19.00 h to 05.00 h and day of mating plug was identified as E0.5. All mouse work was performed under UCSF Institutional Animal Care and Use Committee guidelines in an AAALAC approved facility.

Gonad volumes, germ cell counting and meiotic staging

Gonads were fixed in Bouin's or 4% paraformaldehyde, dehydrated, embedded in paraffin, sectioned at 5 µm, and stained with hematoxylin and eosin (Cancer Diagnostics). Every fifth or tenth section was analyzed for surface area (Histolab) and volumes were extrapolated based on number and thickness. Meiotic staging was based on nuclear shape and chromatin compaction (Abby et al., 2016). Total germ cell counts were obtained from every fourth section, and calculated with Abercrombie's formula correction (Guerquin et al., 2010).

Immunohistochemistry and immunofluorescence

Paraformaldehyde-fixed gonads were embedded in paraffin or OCT (Tissue-Tek). Sections were subjected to heat-mediated antigen retrieval in citrate buffer (pH 6). For immunohistochemistry, endogenous peroxidase activity was inhibited with 3% hydrogen peroxide. For immunohistochemistry and immunofluorescence, sections were blocked in 2% horse serum, incubated with primary antibodies (Table S4) overnight at 4°C, then with peroxidase-conjugated secondary antibody (ImmPRESS™ kit, Vector Laboratories) and DAB (Vector Laboratories) or VIP (Vector Laboratories) or Alexa-Fluor-conjugated secondary antibodies (Invitrogen) and mounted with Vectashield DAPI medium (Vector Laboratories). Imaging was performed

Journal of Cell Science (2016) 129, 2493-2499 doi:10.1242/jcs.189910

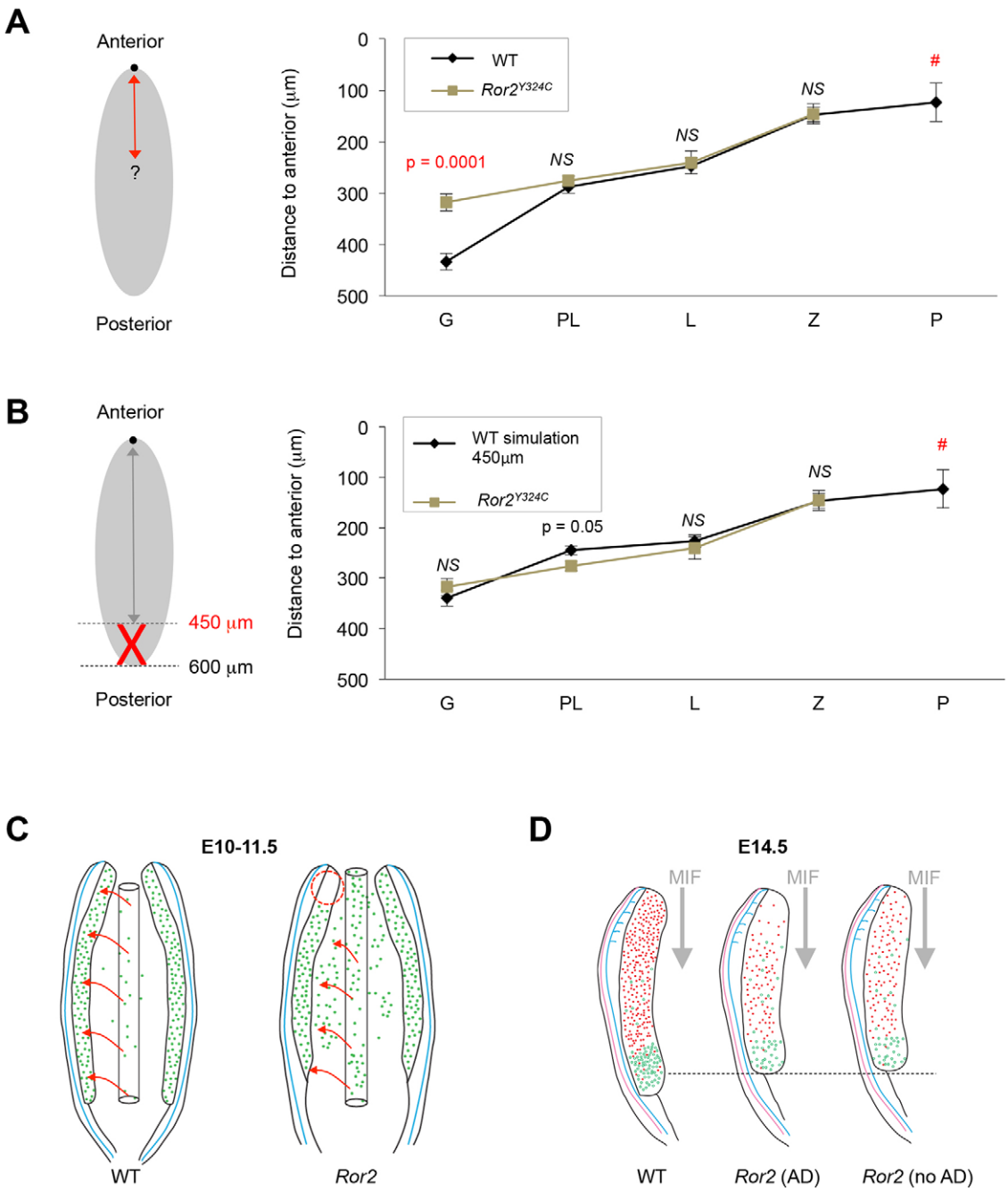

Fig. 4. Anterior loss of germ cells and axial compression of the gonad account for overall meiotic delay in *Ror2* mutants. (A) Comparison of mean measured distance between ovary anterior and meiotic progression of germ cells in *Ror2*^{Y324C} and WT (*n*=6 each). (B) Simulation of axial shortening of *Ror2* gonads using WT dataset. Gono, gonocytes; PL, preleptotene stage; L, leptotene stage; Z, zygotene stage; P, pachytene stage. NS, not significant (*t*-test); #, none detected in Ror^{2Y324C}. Data represented as mean±s.e.m. (C) Model for germ cell migration defects in *Ror2* mutants that lead to the observed anterior defect. Arrows indicate path of germ cell migration from hindgut to the genital ridges. (D) Schematic for meiotic initiation in *Ror2* mutants with and without anterior germ cell defects (AD). Red dots represent germ cells undergoing meiosis whereas green are pre-meiotic germ cells.

using a Leica DM5500 B epifluorescence microscope equipped with CoolSNAP HQ^2 camera (Photometrics) and Leica MMAF software (Metamorph) or Leica SP5 TCS confocal microscope. Images were processed with ImageJ software (NIH) or Volocity (Improvision).

For whole-mount immunofluorescence, gonads were fixed in DMSO: Methanol (1:4) and stained as described (Faire et al., 2015).

RT-qPCR

E12.5 gonads were homogenized in TRIzol (Ambion), followed by RNA extraction (RNeasy Kit, Qiagen), DNAse I treatment, and quantification with NanoDrop (ND-1000). 50 ng of RNA was reverse-transcribed with qScript (Quanta Biosciences). Amplification was carried out with a 1:20 or 1:40 dilution of cDNA (2.5 or 1.25 ng RNA equivalent) on a 7900HT Fast Real-Time PCR System (Applied Biosystems) using primers in Table S5.

Anterior–posterior orientation and quadrant analysis of ovaries

Sagittal sections of Bouin's-fixed ovaries were oriented for anterior–posterior axis (based on positions of the mesonephric ducts) and aligned with gonadal horizontal axis. *XY* coordinates of each germ cell were obtained, such that the abscissa represented distance from a given cell to

Journal of Cell Science

most anterior point in the gonad section. Anterior–posterior axis length was determined (Histolab) and mean length of *Ror2*$^{Y324C/Y324C}$ ovary sections was used for simulation of shortened axis in WT gonads. For quadrant analysis, sections were parsed into four equidistant compartments along the horizontal axis.

Statistics

Statistics were performed in Excel (Microsoft) using the StatPlus plug-in.

Acknowledgements

We thank Svetlana Altshuler-Keylin and Kevin Ebata for feedback on this work.

Competing interests

The authors declare no competing or financial interests.

Author contributions

R.A. and D.J.L. conceived the project. R.A., E.A., A.D.J.R., A.V.C., M.D.K. and V.C. did the experiments. H.-Y.H.H. provided reagents and critical feedback. R.A., E.A., H.-Y.H.H., G.L. and D.J.L. prepared the figures and wrote the manuscript.

Funding

California Institute for Regenerative Medicine [TG TG2-01153] and National Institutes of Health [TG 5T32HD007263-32] to R.A., Irtelis (Commissariat à l'Énergie Atomique et aux Énergies Alternatives) and Fondation ARC pour la Recherche sur le Cancer to E.A., National Science Foundation fellowship to A.V.C., National Institutes of Health diversity supplement [DP2OD007420 S1] to A.D.J.R., University of California, San Francisco Program for Breakthrough Biomedical Research, National Institutes of Health grants [1R21ES023297 and DP2OD007420] and generous philanthropy to D.J.L. and Institut Universitaire de France support to G.L. Deposited in PMC for release after 12 months.

Supplementary information

Supplementary information available online at
http://jcs.biologists.org/lookup/doi/10.1242/jcs.189910.supplemental

References

Abby, E., Tourpin, S., Ribeiro, J., Daniel, K., Messiaen, S., Moison, D., Guerquin, J., Gaillard, J-C, Armengaud, J., Langa, F. et al. (2016). Implementation of meiosis prophase I programme requires a conserved retinoid-independent stabilizer of meiotic transcripts. *Nat. Commun.* **7**, 10324.

Arora, R., Altman, E., Tran, N. D. and Laird, D. J. (2014). Novel domains of expression for orphan receptor tyrosine kinase Ror2 in the human and mouse reproductive system. *Dev. Dyn.* **243**, 1037-1045.

Boiani, M., Kehler, J. and Scholer, H. R. (2004). Activity of the germline-specific Oct4-GFP transgene in normal and clone mouse embryos. *Methods Mol. Biol.* **254**, 1-34.

Bowles, J., Knight, D., Smith, C., Wilhelm, D., Richman, J., Mamiya, S., Yashiro, K., Chawengsaksophak, K., Wilson, M. J., Rossant, J. et al. (2006). Retinoid signaling determines germ cell fate in mice. *Science* **312**, 596-600.

Buehr, M., McLaren, A., Bartley, A. and Darling, S. (1993). Proliferation and migration of primordial germ cells in We/We mouse embryos. *Dev. Dyn.* **198**, 182-189.

Bullejos, M. and Koopman, P. (2004). Germ cells enter meiosis in a rostro-caudal wave during development of the mouse ovary. *Mol. Reprod. Dev.* **68**, 422-428.

Chassot, A.-A., Gregoire, E. P., Lavery, R., Taketo, M. M., de Rooij, D. G., Adams, I. R. and Chaboissier, M. C. (2011). RSPO1/beta-catenin signaling pathway regulates oogonia differentiation and entry into meiosis in the mouse fetal ovary. *PLoS ONE* **6**, e25641.

Chawengsaksophak, K., Svingen, T., Ng, E. T., Epp, T., Spiller, C. M., Clark, C., Cooper, H. and Koopman, P. (2012). Loss of Wnt5a disrupts primordial germ cell migration and male sexual development in mice. *Biol. Reprod.* **86**, 1-12.

DeChiara, T. M., Kimble, R. B., Poueymirou, W. T., Rojas, J., Masiakowski, P., Valenzuela, D. M. and Yancopoulos, G. D. (2000). Ror2, encoding a receptor-like tyrosine kinase, is required for cartilage and growth plate development. *Nat. Genet.* **24**, 271-274.

Di Carlo, A. and De Felici, M. (2000). A role for E-cadherin in mouse primordial germ cell development. *Dev. Biol.* **226**, 209-219.

Douglas, N. C., Arora, R., Chen, C. Y., Sauer, M. V. and Papaioannou, V. E. (2013). Investigating the role of tbx4 in the female germline in mice. *Biol. Reprod.* **89**, 148.

Faire, M., Skillern, A., Arora, R., Nguyen, D. H., Wang, J., Chamberlain, C., German, M. S., Fung, J. C. and Laird, D. J. (2015). Follicle dynamics and global organization in the intact mouse ovary. *Dev. Biol.* **403**, 69-79.

Guerquin, M.-J., Duquenne, C., Lahaye, J.-B., Tourpin, S., Habert, R. and Livera, G. (2010). New testicular mechanisms involved in the prevention of fetal meiotic initiation in mice. *Dev. Biol.* **346**, 320-330.

Hunt, P. A. and Hassold, T. J. (2008). Human female meiosis: what makes a good egg go bad? *Trends Genet.* **24**, 86-93.

Kierszenbaum, A. L. and Tres, L. L. (2001). Primordial germ cell-somatic cell partnership: a balancing cell signaling act. *Mol. Reprod. Dev.* **60**, 277-280.

Koubova, J., Menke, D. B., Zhou, Q., Capel, B., Griswold, M. D. and Page, D. C. (2006). Retinoic acid regulates sex-specific timing of meiotic initiation in mice. *Proc. Natl. Acad. Sci. USA* **103**, 2474-2479.

Koubova, J., Hu, Y.-C., Bhattacharyya, T., Soh, Y. Q., Gill, M. E., Goodheart, M. L., Hogarth, C. A., Griswold, M. D. and Page, D. C. (2014). Retinoic acid activates two pathways required for meiosis in mice. *PLoS Genet.* **10**, e1004541.

Kumar, S., Chatzi, C., Brade, T., Cunningham, T. J., Zhao, X. and Duester, G. (2011). Sex-specific timing of meiotic initiation is regulated by Cyp26b1 independent of retinoic acid signalling. *Nat. Commun.* **2**, 151.

Laird, D. J., Altshuler-Keylin, S., Kissner, M. D., Zhou, X. and Anderson, K. V. (2011). Ror2 enhances polarity and directional migration of primordial germ cells. *PLoS Genet.* **7**, e1002428.

Liu, C.-F., Bingham, N., Parker, K. and Yao, H. H.-C. (2009). Sex-specific roles of beta-catenin in mouse gonadal development. *Hum. Mol. Genet.* **18**, 405-417.

Liu, C.-F., Parker, K. and Yao, H. H.-C. (2010). WNT4/beta-catenin pathway maintains female germ cell survival by inhibiting activin betaB in the mouse fetal ovary. *PLoS ONE* **5**, e10382.

McLaren, A. (2003). Primordial germ cells in the mouse. *Dev. Biol.* **262**, 1-15.

McLaren, A. and Southee, D. (1997). Entry of mouse embryonic germ cells into meiosis. *Dev. Biol.* **187**, 107-113.

Menke, D. B., Koubova, J. and Page, D. C. (2003). Sexual differentiation of germ cells in XX mouse gonads occurs in an anterior-to-posterior wave. *Dev. Biol.* **262**, 303-312.

Molyneaux, K. A., Stallock, J., Schaible, K. and Wylie, C. (2001). Time-lapse analysis of living mouse germ cell migration. *Dev. Biol.* **240**, 488-498.

Naillat, F., Prunskaite-Hyyrylainen, R., Pietila, I., Sormunen, R., Jokela, T., Shan, J. and Vainio, S. J. (2010). Wnt4/5a signalling coordinates cell adhesion and entry into meiosis during presumptive ovarian follicle development. *Hum. Mol. Genet.* **19**, 1539-1550.

Ohkubo, Y., Shirayoshi, Y. and Nakatsuji, N. (1996). Autonomous regulation of proliferation and growth arrest in mouse primordial germ cells studied by mixed and clonal cultures. *Exp. Cell Res.* **222**, 291-297.

Ottolenghi, C., Pelosi, E., Tran, J., Colombino, M., Douglass, E., Nedorezov, T., Cao, A., Forabosco, A. and Schlessinger, D. (2007). Loss of Wnt4 and Foxl2 leads to female-to-male sex reversal extending to germ cells. *Hum. Mol. Genet.* **16**, 2795-2804.

Runyan, C., Gu, Y., Shoemaker, A., Looijenga, L. and Wylie, C. (2008). The distribution and behavior of extragonadal primordial germ cells in Bax mutant mice suggest a novel origin for sacrococcygeal germ cell tumors. *Int. J. Dev. Biol.* **52**, 333-344.

Spiller, C. M. and Bowles, J. (2015). Sex determination in mammalian germ cells. *Asian J. Androl.* **17**, 427-432.

Takeuchi, S., Takeda, K., Oishi, I., Nomi, M., Ikeya, M., Itoh, K., Tamura, S., Ueda, T., Hatta, T., Otani, H. et al. (2000). Mouse Ror2 receptor tyrosine kinase is required for the heart development and limb formation. *Genes Cells* **5**, 71-78.

Vainio, S., Heikkilä, M., Kispert, A., Chin, N. and McMahon, A. P. (1999). Female development in mammals is regulated by Wnt-4 signalling. *Nature* **397**, 405-409.

Warr, N., Siggers, P., Bogani, D., Brixey, R., Pastorelli, L., Yates, L., Dean, C. H., Wells, S., Satoh, W., Shimono, A. et al. (2009). Sfrp1 and Sfrp2 are required for normal male sexual development in mice. *Dev. Biol.* **326**, 273-284.

Yao, H. H.-C, DiNapoli, L. and Capel, B. (2003). Meiotic germ cells antagonize mesonephric cell migration and testis cord formation in mouse gonads. *Development* **130**, 5895-5902.